Effect of Data Reduction and Fiber-Bridging on Mode I Delamination Characterization of Unidirectional Composites

Gretchen B. Murri, NASA Langley Research Center

Submitted for *Proceedings of the American Society for Composites 26th Annual Technical Conference/2nd Joint US-Canada Conference on Composites*

ABSTRACT

Reliable delamination characterization data for laminated composites are needed for input in analytical models of structures to predict delamination onset and growth. The double-cantilevered beam (DCB) specimen is used to measure fracture toughness, G_{Ic}, and strain energy release rate, G_{Imax}, for delamination onset and growth in laminated composites under mode I loading. The current study was conducted as part of an ASTM Round Robin activity to evaluate a proposed testing standard for Mode I fatigue delamination propagation. Static and fatigue tests were conducted on specimens of IM7/977-3 and G40-800/5276-1 graphite/epoxies, and S2/5216 glass/epoxy DCB specimens to evaluate the draft standard "Standard Test Method for Mode I Fatigue Delamination Propagation of Unidirectional Fiber-Reinforced Polymer Matrix Composites." Static results were used to generate a delamination resistance curve, G_{IR}, for each material, which was used to determine the effects of fiber-bridging on the delamination growth data. All three materials were tested in fatigue at a cyclic G_{Imax} level equal to 90% of the fracture toughness, G_{Ic}, to determine the delamination growth rate. Two different data reduction methods, a 2-point and a 7-point fit, were used and the resulting Paris Law equations were compared. Growth rate results were normalized by the delamination resistance curve for each material and compared to the non-normalized results. Paris Law exponents were found to decrease by 5.4% to 46.2% due to normalizing the growth data. Additional specimens of the IM7/977-3 material were tested at 3 lower cyclic G_{Imax} levels to compare the effect of loading level on delamination growth rates. The IM7/977-3 tests were also used to determine the delamination threshold curve for that material. The results show that tests at a range of loading levels are necessary to describe the complete delamination behavior of this material.

Gretchen B. Murri, NASA Langley Research Center, 2 W. Reid St., Hampton, VA 23681, U.S.A

INTRODUCTION

The most common failure mechanism in laminated composite materials is delamination damage. In order to optimize the use of fiber-reinforced composite materials in primary aircraft structures, damage tolerance under static and fatigue loading must be thoroughly understood. Reliable delamination characterization data for laminated composites are needed to use as input in analytical models of structures to predict delamination onset and growth. The double-cantilevered beam (DCB) specimen, as shown in Figs. 1 and 2, is used to measure fracture toughness, G_{Ic}, and strain energy release rate, G_{Imax}, for delamination onset and growth in laminated composites under mode I loading. Reference 1 (ASTM D 5528-01, Standard Test Method for Mode I Interlaminar Fracture Toughness of Unidirectional Fiber-Reinforced Polymer Matrix Composites) presents a standardized test method for measuring static fracture toughness, G_{Ic}. Reference 2 (ASTM D 6115-97, Standard Test Method for Mode I Fatigue Delamination Growth Onset of Unidirectional Fiber-Reinforced Polymer Matrix Composites) is a standardized test method for determining the onset of delamination and a threshold level, G_{Ith}, below which delamination will not start in fatigue. However, there is currently no standard for determining the delamination growth rate in fatigue, once delamination begins. Therefore, a Round Robin test series has been undertaken by ASTM Committee D30 to evaluate a proposed test standard for delamination growth in Mode I specimens under constant amplitude fatigue loading [3]. The work described in this paper was done as part of that Round Robin test series.

For composite materials, delamination growth has typically been related to the cyclic strain energy release rate, G, using a power law expression [4-6], known as the Paris Law. Because the DCB specimen is unidirectional, some nesting of fibers between adjacent plies can occur, resulting in fiber-bridging at the delaminating interface. This fiber-bridging can cause an artificial increase in the measured toughness as the delamination grows [7-8], which will affect the Paris Law curve fit. However, this fiber-bridging is understood to be an artifact of the specimen, and not a material property. In real structures, delaminations typically grow between plies of dissimilar orientation, so fiber-bridging does not occur. Therefore, in order to be useful in structural modeling, expressions relating the delamination growth rate and strain energy release rate must account for the effect of fiber-bridging. Fiber-bridging under quasi-static loading can be quantified as a delamination resistance (G_{IR}) curve, which can be used to correct the growth data for the fiber-bridging effects.

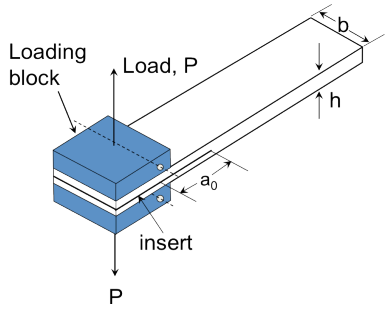

Figure 1. Double-cantilevered beam specimen.

Delamination growth from onset to arrest can be considered to have 3 phases: a region of rapid growth at high (but sub-critical) values of G, a linear growth region, and a slow growth region where the delamination approaches an arrest point, or threshold, below which delamination will not grow. A full-fatigue characterization equation has been proposed [4, 9] to express the complete delamination growth behavior in terms of the maximum cyclic G-value, G_{Imax}; the threshold value, G_{Ith}; and the static fracture toughness, G_{Ic}. In ref. 4 and 5, delamination growth onset data from edge-delamination (EDT) and end-notched flexure (ENF) tests were used to generate threshold curves, below which delamination would not initiate. A minimum threshold for no-delamination-growth was assumed to exist at a loading level for which there was no delamination growth at 1 million cycles.

The objectives of the ASTM Round Robin were to determine the effect of data reduction method and fiber-bridging correction on the delamination growth rate in DCB specimens. Specimens of three different materials were tested. Quasi-static tests were first performed, to determine the fracture toughness, delamination resistance curve, and test parameters for fatigue loading. Fatigue tests were then conducted an initial G_{Imax} level of 90% of G_{Ic}, to determine delamination growth rates, which were expressed in the form of a Paris law. Both a 2-point and a 7-point secant method were used to reduce the delamination growth data and the resulting Paris Law fits were compared. The delamination resistance equations were used to normalize the growth data to account for the effects of fiber-bridging. A Paris Law fit was applied to both the non-normalized and normalized data sets.

An additional objective of this report was to generate a delamination onset curve and a G_{Ith} value, to be used in a full fatigue characterization of one test material, and to compare Paris Law results from tests at different G_{Imax} levels. Additional specimens of that material were therefore tested at 50%, 40%, and 30% of G_{Ic}. The onset of delamination was recorded for these tests and was used to generate a delamination threshold curve for that material. An attempt was made to fit a full fatigue characterization curve to the data, using the complete data set from all G_{Imax} test levels, and the G_{Ic} and G_{Ith} values.

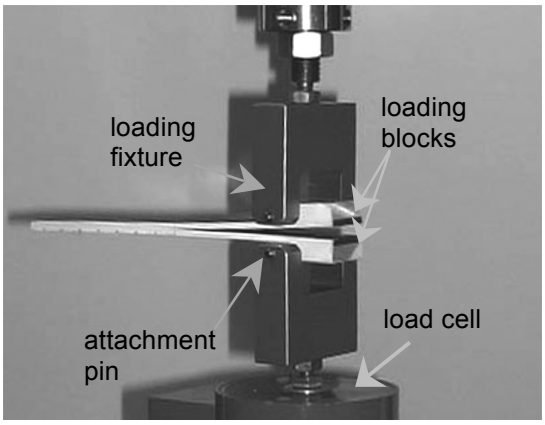

Figure 2. Double-cantilevered beam specimen and loading fixture.

MATERIALS AND SPECIMENS

Three materials were tested: IM7/977-3 and G40-800/5276-1 (carbon/epoxies), and S2/5216 (glass/epoxy.) The IM7/977-3 and G40-800/5276-1 specimens were 26 plies thick and the S2/5216 specimens were 18 plies thick. Cytec Corporation manufactured the panels and cut them into specimens, which were nominally 0.8 inch (20mm) wide and 6-inch (153mm) long. The specimens were received with loading blocks bonded at the insert end of the specimen as a means to apply the opening displacement. A schematic of the DCB specimen is shown in Fig. 1, with the thickness (h), width (w), and initial delamination (a_0) indicated. Prior to testing, specimen dimensions were measured using a micrometer, to the nearest 0.01mm. The average specimen thickness, h, was 0.13 inch (3.4mm) for the IM7/977-3 and G40-800/5276-1 specimens, and 0.16 inch (4.1mm) for the S2/5216 material. The average specimen width, b, was 0.80 inch (20.4mm) for the IM7/977-3 and G40-800/5276-1 specimens, and 0.81 inch (19.7mm) for the S2/5216 material. All specimens were manufactured with a thin PTFE film at the mid-plane at one end. The PTFE insert was 0.0005 inch (13μm) thick and nominally 2.5 inch (63.5mm) long. The initial delamination length, a_0, is the distance from the load-point line to the end of the insert, (see Fig. 1) and was approximately 2.1 inch (53mm.) Specimens were dried before testing, using the procedure in ASTM D5229 [10]. Dried specimens were stored in a dessicator until testing. Immediately before testing, one edge of the specimen was coated with a thin layer of white paint and marked in 1mm increments, starting from the tip of the insert to a length of 60mm.

EXPERIMENTAL PROCEDURES

All tests were conducted under displacement control in a small table-top servo-hydraulic test stand using a 100-lb load cell. A photograph of the test fixture is shown in Fig. 2. The specimens were attached to the test fixtures by means of pins through the loading blocks. The tests were controlled by a computer program, which also recorded the test output data. A 2Megapixel digital camera was used to monitor the delamination growth, and the image was displayed on a computer monitor. Tests were conducted under room temperature conditions. After completing each test, the specimen was split apart at the mid-plane so that the initial delamination length could be more accurately determined, and to verify that the delamination grew evenly across the specimen width.

Static Tests

In order to determine the fracture toughness, G_{Ic}, of each material, quasi-static tests were performed on specimens of each material before fatigue testing. Static tests were also necessary to determine constants for fatigue data reduction and the delamination resistance curve, G_{IR}. Static tests were conducted according to ASTM Standard D5528 [1]. Displacement was applied at a rate of 0.05 in/min (1.27 mm/min.) The computer program recorded load, displacement, and compliance every 0.1 seconds. The camera system recorded a photograph of the specimen edge every 0.5 seconds. Opening displacement, δ, was applied to the specimen until the delamination had grown to at least the 40mm marker.

Fatigue Tests for Delamination Growth Rate

The fatigue tests were conducted according to the specifications of the draft standard, *Standard Test Method for Mode I Fatigue Delamination Propagation of Unidirectional Fiber-Reinforced Polymer Matrix Composites* [3]. Tests were conducted under displacement control, at a frequency of 10 cycles/second. The ratio of minimum displacement to maximum displacement (R-ratio) was $\delta_{min}/\delta_{max}$= 0.1. Prior to fatigue testing, each specimen was loaded quasi-statically, to a maximum displacement that was less than the mean cyclic displacement for that test. This was done in order to determine the initial specimen compliance, and to help verify the location of the insert tip. Under displacement control in fatigue, G_{Imax} decreases from the initial value as the delamination grows. Therefore, the applied G_{Imax} listed for each test is the initial value, and is expressed as a percentage of G_{Ic}. Five specimens of each of the three materials were tested at a cyclic G_{Imax} level equal to 90% of the average G_{Ic} from the static tests. Additional specimens of the IM7/977-3 material were tested at cyclic G_{Imax} values of 50%, 40%, and 30% of G_{Ic}. For each desired G_{Imax} level, maximum cyclic displacement (δ_{max}) for testing was determined from the relationship

$$G_{\mathrm{Imax}} = \frac{\delta_{\max}^2}{\delta_{\mathrm{cr}}^2} G_{Ic} \qquad (1)$$

where δ_{cr} is the average critical displacement from the static tests for each material. The computer system recorded maximum and minimum loads (P), maximum and minimum displacements (δ), compliance (C), and cycle count (N), at every 10 cycles. The camera system recorded a photograph of the specimen edge at every 1000 cycles, taking the photo at the point of maximum cyclic displacement. Specimens were cycled until the delamination growth rate had decreased to at least $1x10^{-7}$ in/cycle ($2.54x10^{-6}$ mm/cycle), or until no growth had been detected by at least $2x10^{6}$ cycles.

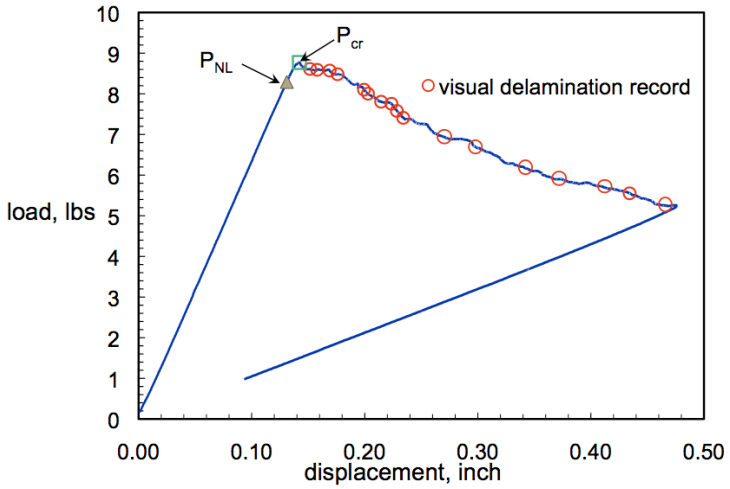

Figure 3. DCB load-displacement plot.

Fatigue Tests for Delamination Onset Threshold

In addition to measuring delamination growth rates, the fatigue tests of the IM7/977-3 specimens were used to determine the delamination onset threshold curve. The test apparatus, specimen preparation, and procedures required by standard 6115 for delamination growth onset (ref. 2) are identical to those specified in the draft standard for delamination growth (ref. 3). Therefore, each IM7/977-3 fatigue test specimen was used to generate both delamination onset data and delamination growth data, by cycling to the onset point (defined as a 1% increase in compliance), and then continuing the fatigue cycling uninterrupted, to generate growth data.

EXPERIMENTAL RESULTS AND DATA REDUCTION

Static Tests

All data reduction was done using the Modified Beam Theory (MBT) method as described in ref. 1, where G_{Ic} is given by

$$G_{Ic} = \frac{3P\,\delta}{2b(a+|\Delta|)} \tag{2}$$

and where P is the load, δ is the displacement, a is the initial delamination length, and Δ is the delamination length correction factor. The fracture toughness was calculated using loads and displacements at the point where the load-displacement curve became nonlinear (G_{NL}), and also at the critical failure point (G_{cr}). Figure 3 shows an example of a typical load-displacement curve, with the non-linear and critical points indicated. The relationship between the compliance and delamination length for the MBT solution is

$$C^{1/3} = m(a+|\Delta|) \tag{3}$$

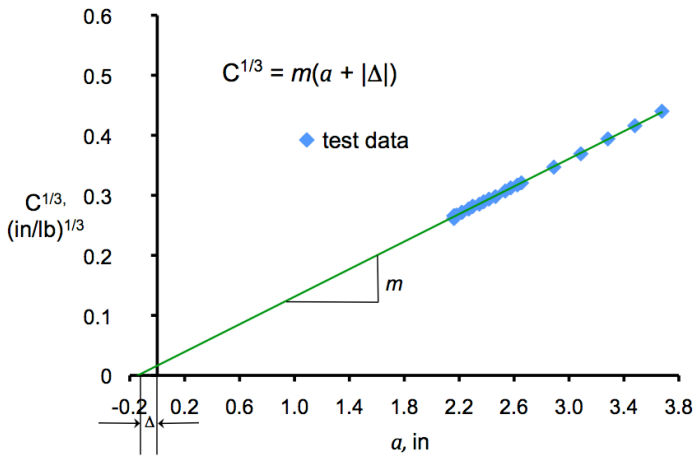

Figure 4. Static DCB compliance calibration plot.

For each specimen, the constants *m* and Δ were determined by plotting the observed delamination lengths from the static test vs. the cube root of the corresponding compliance, and applying a least squares line fit, as shown in Fig. 4. For each material, the values of *m* and Δ for all specimens were then averaged, to determine *m* and Δ to use in the fatigue data reduction.

Static G_{Ic} results for all three materials are shown in Table I. Results for the IM7/977-3 and G40-800/5276-1 materials were fairly consistent between the specimens, with Coefficients of Variation of approximately 7 to 8% for the G_{NL} values and 4 to 5% for the G_{cr} values. There was greater variation in the S2/5216 material, which had Coefficients of Variation of approximately 19 and 17%, for G_{NL} and G_{cr}.

TABLE I. STATIC DCB DATA

Material	G_{Ic}^{NL}, in - lb/in^2, (J/m^2)	G_{Ic}^{cr}, in - lb/in^2, (J/m^2)	m, (in/lb)$^{1/3}$/in, ((mm/N)$^{1/3}$/mm)	Δ, in (mm)
IM7/977-3	0.88 (154.2)	1.02 (178.7)	0.1114 (7.84x10^{-3})	-0.1899 (-4.82)
G40-800/5276-1	1.67 (292.6)	1.93 (338.1)	0.1174 (8.26x10^{-3})	-0.1549 (-3.93)
S2/5216	0.91 (159.4)	1.15 (201.5)	0.1271 (8.94x10^{-3})	-0.4013 (-10.19)

Fiber-bridging was observed in the static testing, particularly in the S2/5216 specimens. Figure 5 shows a photograph of an S2/5216 specimen during static testing, showing the extensive fiber-bridging. A main objective of the ASTM Round Robin was to evaluate the effect of fiber-bridging on fatigue delamination growth and the Paris Law. Therefore, the static test results were used to determine a delamination resistance curve equation, (R-curve) for each material, to be used in the fatigue data reduction. During the static testing, after the critical displacement point was reached, opening displacement was continued, and G_I was calculated as the delamination continued to grow. The calculated G-values were plotted vs. the delamination length to produce the R-curve. Increasing values of G_I as the delamination grows indicate fiber-bridging is likely to be occurring in the specimen.

The IM7/977-3 specimens showed an increasing R-curve from initiation until the delamination had grown approximately 0.2 inches (5.1mm), where G_I reached a plateau level of 1.14 in-lb/in^2 (199.7 J/m^2). The G40-800/5276-1 specimens showed an approximately linear R-curve throughout the test, for delamination

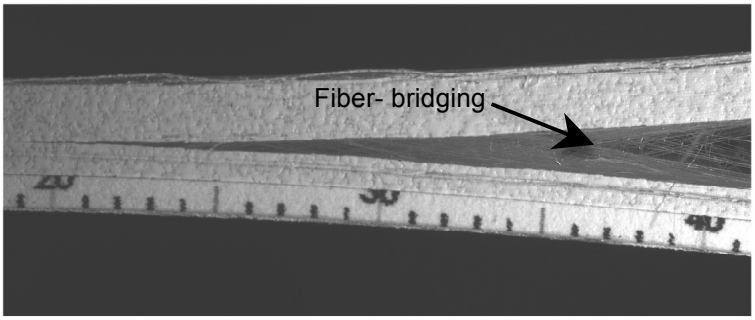

Figure 5. Fiber-bridging in S2/5216 DCB specimen.

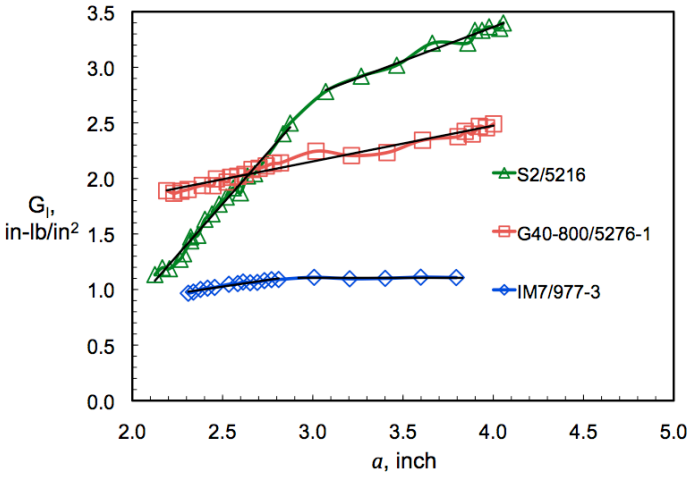

Figure 6. Delamination resistance curves.

growth of 2 inches (50.8mm), with no plateau level observed. The S2/5216 specimens also showed an increasing R-curve throughout the loading, with a constant slope for the first 1-inch (25.4mm) of delamination growth, followed by another linear region, with a different slope, over the final 1.5 inches (38.1mm) of delamination growth. An example R-curve from each material type is shown in Fig. 6. The amount of fiber-bridging observed in the tests corresponded to the steepness of the curves in Fig. 6, with the S2/5216 showing extensive fiber-bridging, and the two carbon/epoxies exhibiting very little.

An expression for delamination resistance (G_{IR} equation) can be generated from the static test data. For each material type, all the static results of that material were plotted together, and an appropriate equation was fit to the complete data set. The expressions for each material are given in Table II. Under fatigue loading, delaminations did not grow beyond a=2.6 inch (66mm) for the IM7/977-3 specimens, or beyond a=3.0 inch (76.2mm) for the S2/5216 specimens, so that only the first part of the G_{IR} expressions were needed for the data reduction.

TABLE II. DELAMINATION RESISTANCE CURVE EXPRESSIONS

Material	G_{IR}, in-lb/in^2
IM7/977-3	0.2363a+0.5504, for a<2.6 inch; 1.16 for a>2.6 inch
G40-800/5276-1	0.1846a+1.458 for a<4.0 inch
S2/5216	2.141a-3.558, for a<3.0; 0.9142a - 0.1051 for a>3.0

Delamination Onset

In addition to the specimens tested at 90% G_{Ic}, specimens of the IM7/977-3 material were cycled at G_{Imax} levels of 50%, 40%, and 30% G_{Ic}, to determine a threshold curve for no delamination onset. As specified by ref. 2, the onset of delamination in each specimen is defined as the point at which the compliance increases by 1%. The initial G_{Imax} of the test is plotted vs. the number of loading cycles to the 1% C increase point. Tests are conducted at a range of G_{Imax} levels, to

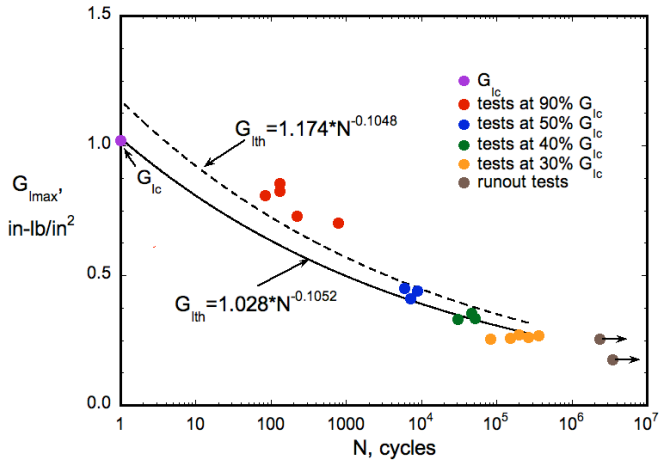

Figure 7. Delamination onset for IM7/977-3 DCB specimens.

generate the delamination onset curve shown in Fig. 7. The average fracture toughness, G_{Ic}, is also plotted on Fig. 7, at N=1. Results at the lower G_{Imax} levels are consistent for each load level, but the 90% values are more scattered. The two tests at the highest cycle counts are shown with right-pointing arrows, indicating that these are run-out tests, for which no delamination growth occurred.

Delamination growth was verified in all the specimens by splitting them apart and inspecting the midplane surface after completion of the delamination growth testing. At the 30% G_{Ic} level, there is a wider range of N_{onset} values, and one specimen was a run-out. These specimens all showed very little delamination growth at the midplane (less than 0.125 inch) during post-test inspection. For the IM7/977-3 specimens, therefore, the threshold for no-delamination-growth appears to be near 30% G_{Ic}.

Typically, a power curve is fit through this data set, to give a threshold below which delamination should not occur [4, 5]. A curve was fit first through the complete data set. This is shown by the dashed line in Fig. 7, along with the corresponding equation. A second equation, shown by the solid line, was fit through the data at the lower G_{Imax} values only (ignoring the 90% G_{Imax} data.) Both curves predict delamination onset in the 90% tests at lower cycle counts than were measured in the tests. Because the lower curve fit (solid line) was a better fit to the G_{Ic} value, and because it is more conservative, it was used to calculate a threshold value, G_{Ith}, at N=1x10^6 cycles, equal to 0.24 in-lb/in^2 (42.1 J/m^2).

Delamination Growth at G_{Imax}=90%G_{Ic}

Specimens of each material were cyclically loaded at G_{Imax}=90%G_{Ic} to generate delamination growth data. Testing was typically conducted until the growth rate, da/dN, decreased to 1x10^{-7} in/cycle (2.54x10^{-6} mm/cycle), but in some cases was continued beyond that point.

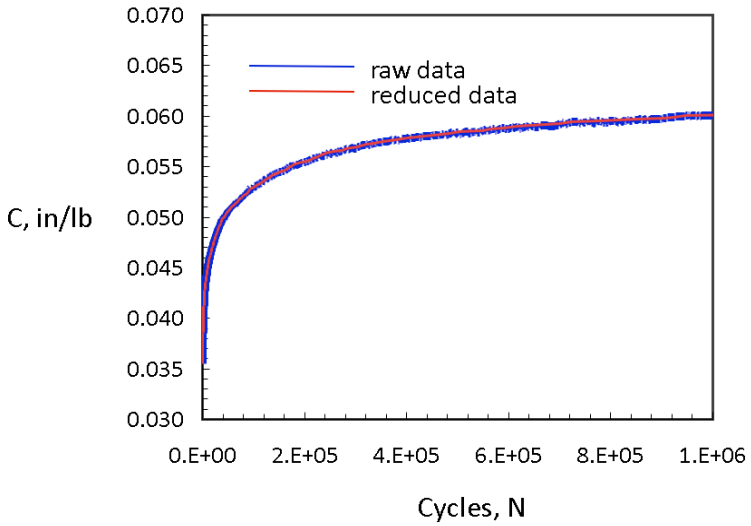

Figure 8. Effect of data parsing on compliance curve.

Before calculating the delamination growth rate, da/dN, a parsing routine was applied to the very large raw data files to eliminate scatter and reduce the data set to a more manageable size. This parsing routine compared the change in delamination length for each pair of consecutive data lines to a pre-set limit, and eliminated data points for which the delamination length increase was less than this limit. Figure 8 shows an example of C vs. N for the raw data set and for the reduced data set. The delamination length, a, at each data point, was calculated from eq. (3), using the average values of m and Δ from the static testing, as shown in Table I, and the compliance data at that point. The reduced data and raw data are in excellent agreement. Figure 9 shows a plot of a vs. N for two different specimens of IM7/977-3, showing visually observed values of a, determined from the

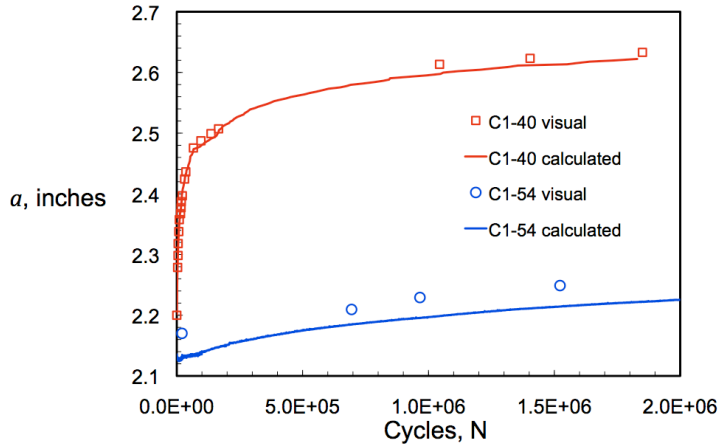

Figure 9. Comparison of calculated and measured delamination length.

automated photographs, and the calculated values. For the C1-40 specimen, the agreement between calculated and visually observed values is very good, although there is some difference at the high cycle counts. For the C1-54 specimen, there is a small offset between the measured and calculated values of *a*, however, the data follows the same trend. The calculated values of *a* were used for all the data reduction.

To determine the delamination growth rate, d*a*/dN, the draft standard [3] recommends two data reduction methods, a 2-point method, and a 7-point secant method. These calculations were applied to the reduced data sets for all specimens. For the 2-point method, d*a*/dN is determined from the slope of the line between two adjacent points on the plot of *a* (delamination length) vs. N (cycle count.) The corresponding value of G_{Imax} is calculated from eq. (2),

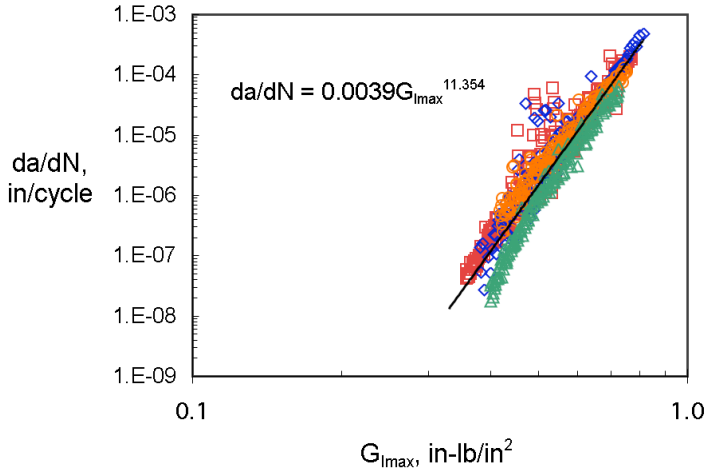

(a) Delamination growth data with 2-point fit data reduction.

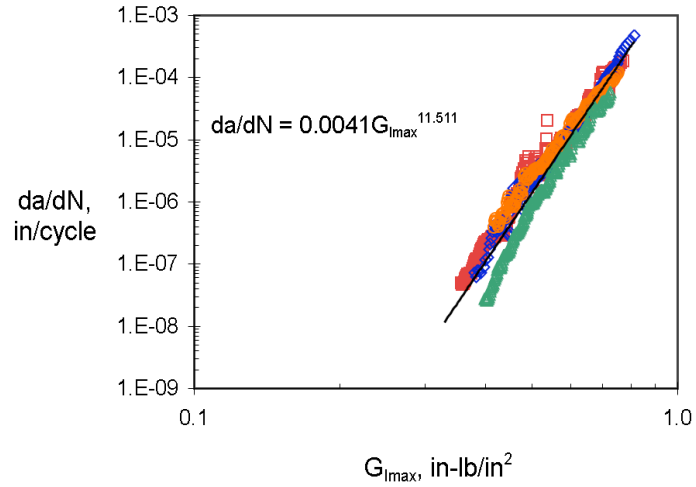

(b) Delamination growth data with 7-point fit data reduction.

Figure 10. Comparison of 2-point and 7-point secant fit data reductions for S2/5216.

where a and P are the averaged values from the two data points. The 7-point secant method calculates da/dN by fitting a second order polynomial to sets of 7 successive data points. A complete description of this method can be found in ASTM Standard E647-00 [11].

Figure 10 shows G_{Imax} vs. da/dN for both the 2-point and 7-point calculation methods for the S2/5216 material, where the colors represent the different specimens. The results show good repeatability between the specimens, but there is noticeably more scatter in the 2-point reduced data. A Paris Law expression of the form da/dN=A(G_{Imax}^{B}), where B reflects the slope of the line, was fit to the 2-point and 7-point results for each specimen. Comparing the exponents, B, for each calculation method showed a difference of typically 1% or less for any specimen. This comparison was repeated for the other two materials, with similar results. The maximum difference between the power law exponents was 2.4% for all specimens tested. Figures 11-12 show G_{Imax} vs. da/dN from the 7-point secant method, for the

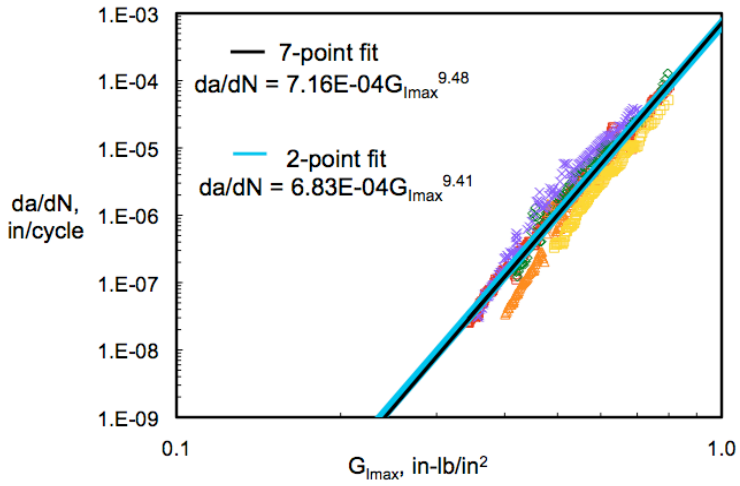

Figure 11. Delamination growth curve for IM7/977-3 specimens at 90%G_{Ic}.

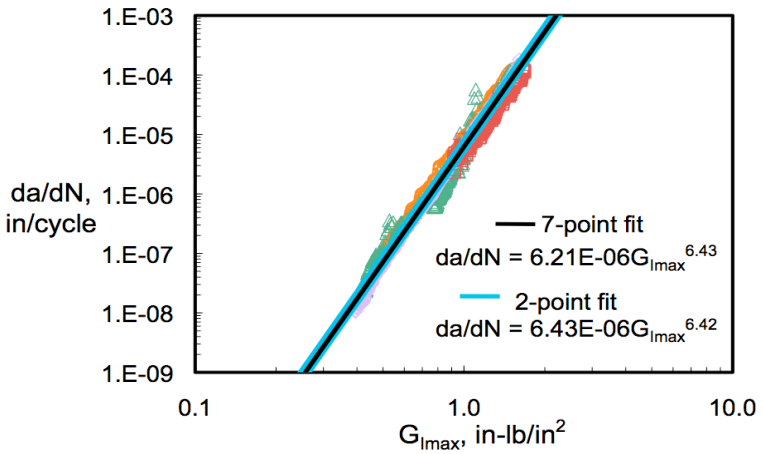

Figure 12. Delamination growth curve for G40-800/5276-1 DCB specimens.

IM7/977-3 and G40-800/5276-1 materials, respectively. The IM7/977-3 results in Fig. 11 are only those for the IM7/977-3 specimens tested at G_{Imax}=90%G_{Ic}, not those tested at the lower G_{Imax} levels. Results for these materials show good repeatability. In Figs. 11 and 12, the Paris Law has been fit to the complete data set (using 7-point secant data reduction) and is shown on the plot. The Paris Law equation from the 2-point data reduction is also shown on each figure for comparison and is within 1.4% for all the materials. Therefore, the 7-point solution method was considered to accurately represent the delamination growth, with less scatter, and was used in the remainder of the data reduction, rather than the 2-point method.

Fiber-bridging and Normalized G_{Imax}

In order to evaluate the contribution of fiber-bridging to the delamination growth results, the G_{Imax} data in Figs. 10b, 11, and 12 were normalized by the appropriate G_{IR} expressions from Table II. However, since G_{Imax}/G_{IR} has no units, those values were multiplied by G_{Ic} for each material to allow comparison with the non-normalized G_{Imax} results. The normalized results are shown in Figs. 13-15, along with the non-normalized results for the complete data sets for each material. The values of A and B from the Paris Law fits, both with and without the G_{IR} correction applied, are shown in Table III.

TABLE III. NON-NORMALIZED AND NORMALIZED PARIS LAW CONSTANTS

Material	$da/dN=A(G_{Imax})^B$			
	A, non-normalized	B, non-normalized	A, normalized	B, normalized
IM7/977-3 (90%G_{Ic} tests)	7.91E-04	9.63	8.53e-4	8.57
G40-800/5276-1	6.21E-06	6.43	5.49E-06	6.08
S2/5216	4.13E-03	11.51	1.30E-03	6.19

A comparison of the original and normalized B-values for each material shows decreases of 11.01%, 5.44%, and 46.22% for the IM7/977-3, G40-800/5276-1, and S2/5216 materials, respectively. The magnitude of the reduction corresponds to the amount of fiber-bridging that was observed in the testing, with G40-800/5276-1 showing minimal fiber-bridging, and S2/5216 showing extensive fiber-bridging. A comparison of the data sets in Fig. 15 shows that, at a given applied G_{Imax} level, the growth rate is faster for the normalized data than indicated by the non-normalized results. As the delamination grows and the amount of fiber-bridging increases, the difference between non-normalized and normalized growth rate is more than an order of magnitude for the S2/5216 material. The value of A also changes in the normalized results, which is reflected in Figs. 13 and 15 by the shift of the data to the left. Figures 13 and 15 show that the delamination arrest points for those materials are at lower values of G_{Imax} than would be indicated by the non-normalized results.

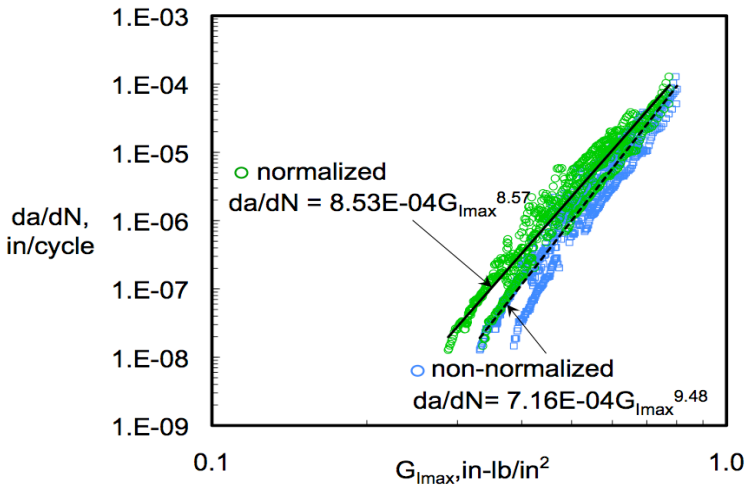

Figure 13. Normalized and non-normalized Paris Laws for IM7/977-3 specimens tested at 90%G_{Ic}.

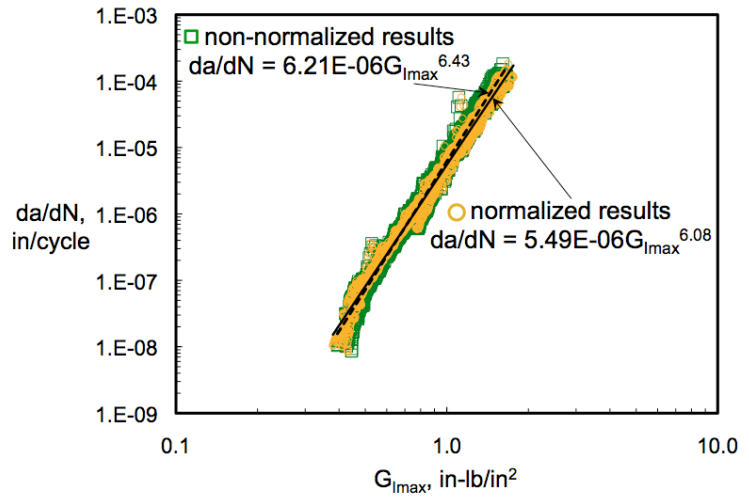

Figure 14. Normalized and non-normalized Paris Laws for G40-800/5276-1 specimens.

Reference 12 also presents results from the Round Robin testing. In that study, values of B from the normalized data were found to be 6.82, 6.31, and 5.5; representing decreases of 18%, 9.5%, and 44% for the IM7/977-3, G40-800/5276-1, and S2/5216 materials, respectively. Although the exponent values in the current study differ somewhat from ref. 12, the magnitude of the reduction due to normalizing the data is similar.

As Figs. 13 and 15 demonstrate, the effect of fiber-bridging on measured delamination growth rate can be significant. In a structure where delamination is the dominant failure mode, this difference must be recognized and accounted for in the design process.

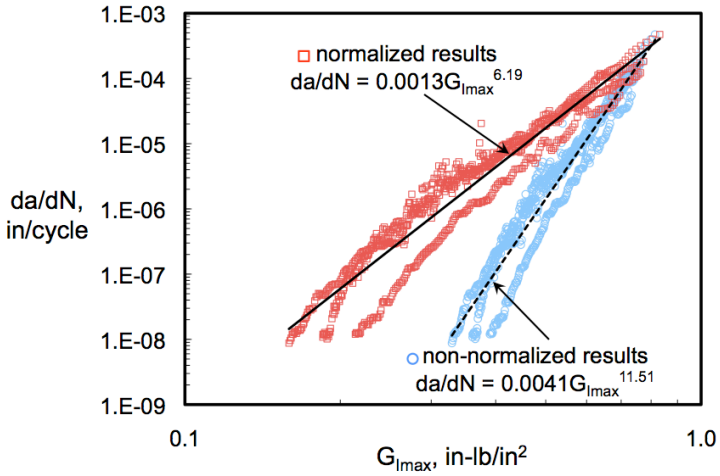

Figure 15. Normalized and non-normalized Paris Law for S2/5216 specimens.

Delamination Growth in IM7/977-3 at a Range of G_{Imax} levels

Delamination growth rates were also calculated for the IM7/977-3 fatigue specimens tested below 90% G_{Ic}. Figure 16 shows G_{Imax} vs. da/dN for the complete data set, with each specimen represented by a different color. Figure 17 shows the normalized data for the same specimens, where the specimens are grouped by G_{Imax} levels. The slopes of most of the data sets are similar to the 90% G_{Ic} results, although the position of the curves shifts to the left with decreasing G_{Imax} levels. Also, for tests at G_{Imax} of 90%, 40%, and 30%, the data at the lower end appear to be changing slope and tending toward becoming vertical. This would indicate that the delamination growth is arresting at a different G-value for each loading level. The load rate at which this change of slope occurs is approximately da/dN=1x10^{-8} inch/cycle (2.54x10^{-7} mm/cycle) for all the load levels. The tests at 50% G_{Ic} were not continued long enough to reach a turning point in the slope of the data. The results for the specimens tested at 50%, 40%, and 30% are shown in Fig. 18-20, respectively. Because the initial growth rate for the tests at 40% and 30%

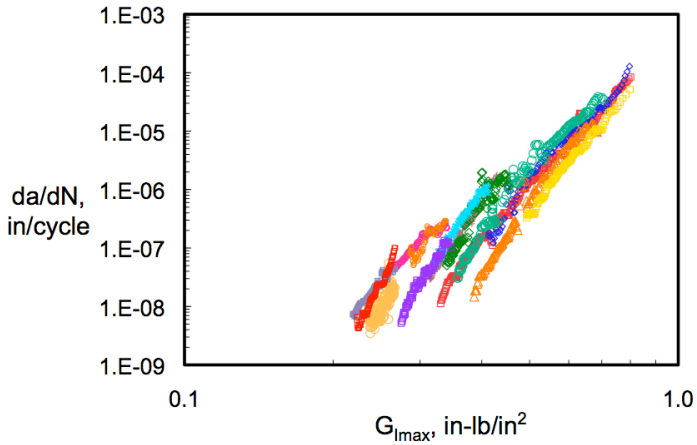

Figure 16. Delamination growth data for IM7/977-3 material at four G_{Imax} levels.

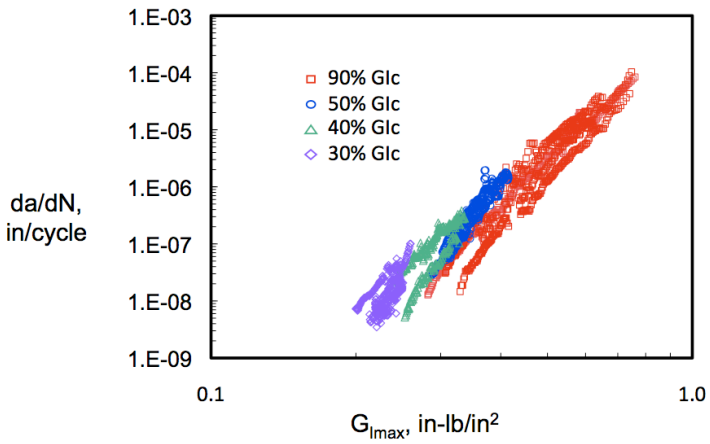

Figure 17. Normalized delamination growth results for IM7/977-3 specimens.

was less than $7x10^{-6}$ in/cycle ($1.78x10^{-4}$ mm/cycle), testing of these specimens was allowed to continue beyond da/dN=$1x10^{-7}$ in/cycle ($2.54x10^{-6}$ mm/cycle). Figure 18 shows excellent repeatability among the 50% specimens. Figure 19 shows that there is slightly more variability in the 40% results. The results at 30% G_{Ic} are shown in Fig. 20. These tests showed the greatest variability in the results. The data sets at this level are almost vertical in some cases, with da/dN starting no higher than $1x10^{-7}$ inch/cycle ($2.54x10^{-6}$ mm/cycle) and rapidly decreasing. The threshold value of G_{Imax} from the onset tests (G_{Ith}) is also shown on the plot. For all the specimens shown, the G_{Imax} at which delamination started was higher than the calculated threshold value. The Paris Law equations for the 50% and 40% data sets are shown on Figs. 18 and 19, where the exponents are 10.6 and 9.2, respectively. These values are consistent with each other, but are slightly higher than the 90% G_{Ic} normalized value of 8.44 for the IM7/977-3 material.

In Fig. 21, the Paris Law is fit to the combined IM7/977-3 normalized data from all loading levels. The exponent was found to be 7.16, lower than any of the values from the individual load levels, due to the leftward shifting of the data sets at the different load levels.

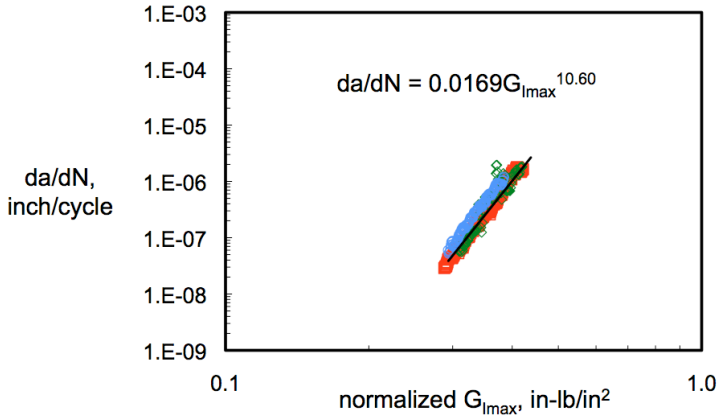

Figure 18. Delamination growth in IM7/977-3 specimens at G_{Imax}=50%G_{Ic}.

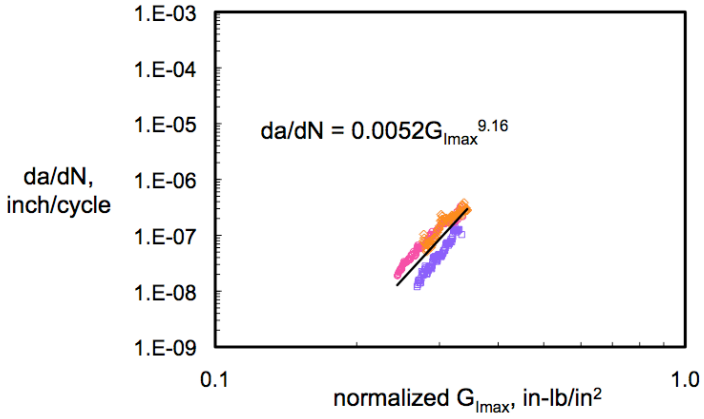

Figure 19. Delamination growth in IM7/977-3 specimens at G_{Imax}=40%G_{Ic}.

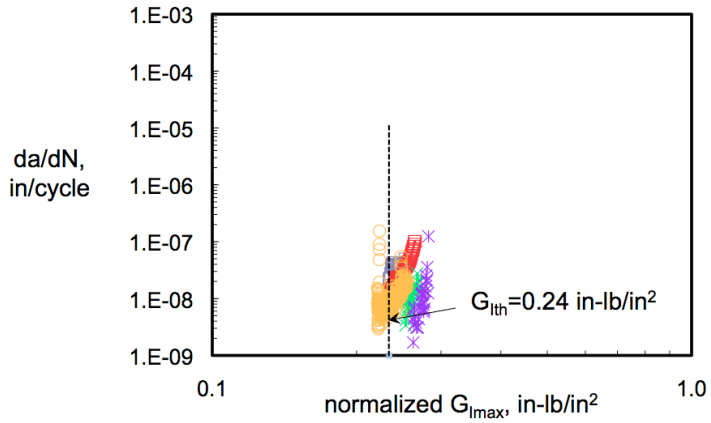

Figure 20. Delamination growth in IM7/977-3 specimens at G_{Imax}=30%G_{Ic}.

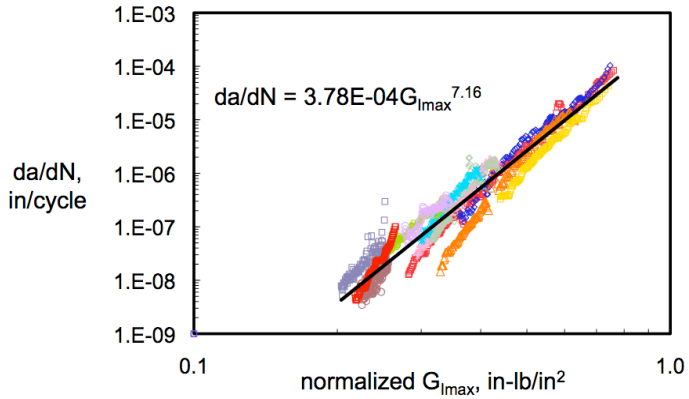

Figure 21. Paris Law fit to combined IM7/977-3 DCB data.

The Paris Law fit from each load level was used to calculate the value at which delamination will arrest, using a value of da/dN=1x10^{-8} in/cycle (2.54x10^{-7} mm/cycle), the approximate value where the onset curves tended to become vertical, along with the normalized Paris Law expressions on Figs. 13, 18, 19, and 21. For the 90%, 50%, 40%, and complete data sets, the delamination arrest values were 0.231, 0.237, 0.31, and 0.229 in-lb/in^2 (40.5, 41.5, 54.3, and 40.1 J/m^2), respectively, compared to the G_{Ith} value of 0.240 in-lb/in^2 (42.1 J/m^2) from the onset data curve fit, at N=1x10^6 cycles.

Full Fatigue Characterization

In refs. 4, 5, and 9, the following equation was postulated as a way to characterize the complete fatigue delamination behavior of a composite material, from onset to delamination arrest:

$$\frac{da}{dN} = A(G_{\max})^B \left[\frac{1-\left(\frac{G_{th}}{G_{\max}}\right)^{D1}}{1-\left(\frac{G_{\max}}{G_c}\right)^{D2}} \right] \tag{4}$$

The constants A and B are those from the Paris Law fit to the normalized data, and the constants D1 and D2 are determined from fitting eq. (4) to the experimental data. In Fig. 22, eq. (4) has been fit separately to the 90%, 50%, and 40% data sets, and to the complete data set, using G_{Ic} from Table I and G_{Ith}=0.24 in-lb/in^2. Each curve is shown on the figure along with the data from all G_{Imax} levels. As the figure shows, the 90% data predicts that the delamination will slow down faster, and arrest at a higher value of G_I, than predicted by the 50% and 40% tests. The curve fits to the data from 40% and 50% G_{Imax} tests predict higher initial growth rates for the 90% tests than was actually measured. For these IM7/977-3 specimens, an accurate full fatigue curve that describes the complete data set could not be generated using delamination growth data from only one load level.

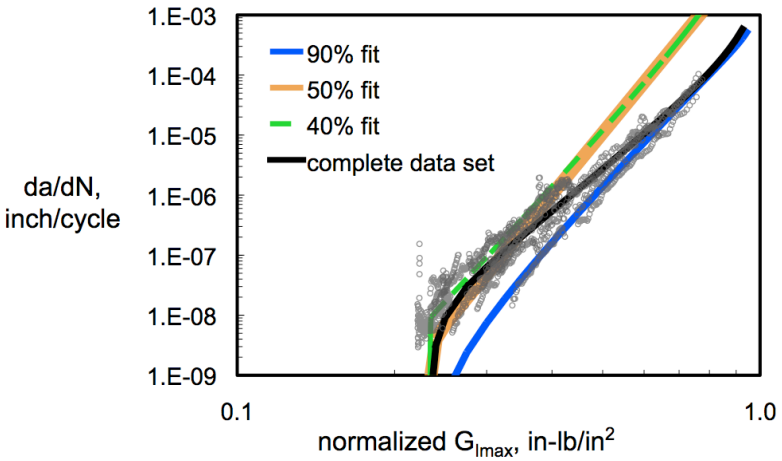

Figure 22. Full fatigue characterization curve for IM7/977-3 DCB specimens.

SUMMARY

Static and fatigue tests were conducted on specimens of IM7/977-3 and G40-800/5276-1 graphite/epoxies, and S2/5216 glass/epoxy double-cantilevered beam specimens as part of an ASTM Round Robin to evaluate the draft standard "Standard Test Method for Mode I Fatigue Delamination Propagation of Unidirectional Fiber-Reinforced Polymer Matrix Composites." Static results were used to generate a delamination resistance curve, G_{IR}, for each material, which was used to determine the effects of fiber-bridging on the delamination growth data. All three materials were tested in fatigue at a cyclic G_{Imax} level equal to 90% of the fracture toughness, G_{Ic}, to determine the delamination growth rate. Two different data reduction methods, a 2-point and a 7-point fit, were used and the resulting Paris Law equations were compared. Growth rates were plotted vs. the applied G_{Imax}, and vs. the normalized G_{Imax}, which was determined by dividing G_{Imax} by the delamination resistance curve. Additional specimens of the IM7/977-3 material were tested at 3 lower cyclic G_{Imax} levels to compare delamination growth rates. The IM7/977-3 tests were also used to determine the delamination threshold curve for that material. The following observations were made:

1. There was very little difference in the Paris Law results using the 2-point and 7-point data reduction methods. The 7-point method was considered better because of reduced scatter in the resulting plots.

2. The Paris Law exponents for the normalized growth plots were from 5% to 47% lower than for the non-normalized plots, depending on the amount of fiber-bridging in the material type. In a material with extensive fiber-bridging in the DCB test, actual delamination growth rates without fiber-bridging will be significantly faster than indicated by the non-normalized results. Therefore, fiber-bridging must be accounted for in assessing the delamination behavior of a material.

3. An attempt was made to generate a full fatigue characterization curve for the IM7/977-3 material, using the test values of G_{Ic} and G_{Ith} and the complete data set from all G_{Imax} test levels. The result is compared to similar curve fits calculated using growth data from only one load level. The results show that tests at a range of loading levels are necessary to describe the complete delamination behavior of this material.

REFERENCES

1. "ASTM D 5528-01, Standard Test Method for Mode I Interlaminar Fracture Toughness of Unidirectional Fiber-Reinforced Polymer Matrix Composites," in *Annual Book of ASTM Standards*. Vol. 15.03, American Society for Testing and Materials, 2008.

2. "ASTM D 6115-97, Standard Test Method for Mode I Fatigue Delamination Growth Onset of Unidirectional Fiber-Reinforced Polymer Matrix Composites," in *Annual Book of ASTM Standards*. Vol. 15.03, American Society for Testing and Materials, 2008.

3. "Standard Test Method for Mode I Fatigue Delamination Propagation of Unidirectional Fiber-Reinforced Polymer Matrix Composites," Draft standard, ASTM International, Committee

D30 on Composites, 2009.

4. Martin, R. H., and Murri, G. B., "Characterization of Mode I and Mode II Delamination Growth and Thresholds in AS4/PEEK Composites," *Composite Materials: Testing and Design (Ninth Volume), ASTM STP 1059*, S. P. Garbo, Ed., American Society for Testing and Materials, Philadelphia, 1990, pp. 251-270.

5. O'Brien, T. Kevin, "Towards a Damage Tolerance Philosophy for Composite Materials and Structures," *Composite Materials: Testing and Design (Ninth Volume), ASTM STP 1059*, S. P. Garbo, Ed., American Society for Testing and Materials, Philadelphia, 1990, pp. 7-33.

6. Russell, A. J., and Street, K. N., "A Constant ΔG Test for Measuring Mode I Interlaminar Fatigue Crack Growth Rates," *Composite Materials: Testing and Design (Eighth Conference), ASTM STP 972*, J. D. Whitcomb, Ed., American Society for Testing and Materials, Philadelphia, 1988, pp. 259-277.

7. Johnson, W. S., and Mangalgiri, P. D., "Investigation of Fiber Bridging in Double Cantilever Beam Specimens," Journal of Composites Technology and Research, Vol. 9, No. 1, Spring 1987, pp.10-13.

8. Poursartip, Anoush, "Characterization of Edge Delamination Growth in Laminates Under Fatigue Loading," *Toughened Composites, ASTM STP 937*, Norman J. Johnston, Ed., American Society for Testing and Materials, Philadelphia, 1987, pp. 222-241.

9. Shivakumar, K., Chen, H., and Abali, F, "A Total Fatigue Life Model for Mode I Loaded Composite Laminates," *International Journal of Fatigue*, Vol. 28, Issue 1, January 2006, pp. 33-42.

10. "ASTM D 5229/D 5229 M-92, Standard Test Method for Moisture Absorption Properties and Equilibrium Conditioning of Polymer Matrix Composite Materials," in *Annual Book of ASTM Standards*. Vol. 15.03, American Society for Testing and Materials, 2008.

11. "ASTM E 647-00, Standard Test Method for Measurement of Fatigue Crack Growth Rates," in *Annual Book of ASTM Standards*. Vol. 03.01, American Society for Testing and Materials, 2000.

12. Giannis, S., Hansen, K., and Martin, R. H., "Accounting for the R-curve Effects on the Mode I Fatigue Delamination Growth Characterisation of Unidirectional Composites," *Proceedings of the American Society for Composites*, Twenty-fifth Technical Conference, September 20-22, 2010, Dayton, Ohio.

ACKNOWLEDGEMENTS

The author would like to thank ASTM Committee D30 and Cytec Materials for supplying test specimens for this project. Appreciation is also expressed to Mr. William Johnston, of Lockheed Martin, for his assistance with the data parsing routine, and Mr. Richard Churray, of NASA Langley, for his assistance in conducting the tests.